Development 130, 4235-4248

doi:10.1242/dev.00625

Consequences of the depletion of zygotic and embryonic enhancer of zeste 2 during preimplantation mouse development

Sylvia Erhardt[1,2], I-hsin Su[3], Robert Schneider[1], Sheila Barton[1], Andrew J. Bannister[1], Laura Perez-Burgos[4], Thomas Jenuwein[4], Tony Kouzarides[1], Alexander Tarakhovsky[3,*] and M. Azim Surani[1,†]

[1]Wellcome Trust/Cancer Research UK Institute, University of Cambridge, Tennis Court Road, Cambridge CB2 1QR, UK
[2]LBNL, MS 84-171, 1 Cyclotron Road, Berkeley, CA 94720, USA
[3]Laboratory of Lymphocyte Signaling, the Rockefeller University, 1230 York Avenue, New York, NY 10021, USA
[4]IMP, Dr. Bohrgasse 7, A-1030 Vienna, Austria
*To whom requests for mice carrying conditional Ezh2 allele should be sent
†Author for correspondence (e-mail: as10021@mole.bio.cam.ac.uk)

Accepted 23 May 2003

SUMMARY

Enhancer of zeste 2 (Ezh2), a SET domain-containing protein, is crucial for development in many model organisms, including early mouse development. In mice, Ezh2 is detected as a maternally inherited protein in the oocyte but its function at the onset of development is unknown. We have used a conditional allele of *Ezh2* to deplete the oocyte of this maternal inheritance. We show that the loss of maternal Ezh2 has a long-term effect causing severe growth retardation of neonates despite 'rescue' through embryonic transcription from the paternal allele. This phenotypic effect on growth could be attributed to the asymmetric localisation of the Ezh2/Eed complex and the associated histone methylation pattern to the maternal genome, which is disrupted in *Ezh2* mutant zygotes. During subsequent development, we detect distinct histone methylation patterns in the trophectoderm and the pluripotent epiblast. In the latter where *Oct4* expression continues from the zygote onwards, the Ezh2/Eed complex apparently establishes a unique epigenetic state and plasticity, which probably explains why loss of Ezh2 is early embryonic lethal and obligatory for the derivation of pluripotent embryonic stem cells. By contrast, in the differentiating trophectoderm cells where *Oct4* expression is progressively downregulated Ezh2/Eed complex is recruited transiently to one X chromosome in female embryos at the onset of X-inactivation. This accumulation and the associated histone methylation are also lost in *Ezh2* mutants, suggesting a role in X inactivation. Thus, Ezh2 has significant and diverse roles during early development, as well as during the establishment of the first differentiated cells, the trophectoderm, and of the pluripotent epiblast cells.

Supplemental data available online

Key words: Polycomb, Ezh2, Histone methylation, X-inactivation, Pluripotency, Mouse

INTRODUCTION

Polycomb group (PcG) proteins are involved in heritable epigenetic regulation of gene expression during development (Paro and Harte, 1996). Among these PcG genes are enhancer of zeste 2 (*Ezh2*) and its interacting partner embryonic ectoderm development (*Eed*) which are essential for early development in most model organisms (Abel et al., 1996; Chen et al., 1996; Hobert et al., 1996; Sewalt et al., 1998). They are also the most highly conserved PcG genes throughout evolution, and the only known members in *Caenorhabditis elegans*, where they are essential in the germ line (Seydoux and Strome, 1999). The Ezh2 homologue in *Arabidopsis*, Medea, is maternally inherited and crucial for development (Grossniklaus et al., 1998).

There are two mammalian homologues of enhancer of zeste: *Ezh1*, which is expressed predominantly in adult tissues, and *Ezh2*, which is expressed primarily in early development (Laible et al., 1997). Mutations of *Ezh2* and *Eed* are very early embryonic lethal (Faust et al., 1998; O'Carroll et al., 2001; Schumacher et al., 1996). *Ezh2* is also essential for the derivation of pluripotent embryonic stem (ES) cells (O'Carroll et al., 2001), and it is upregulated in prostate cancer (Varambally et al., 2002). Furthermore, Ezh2 and Eed are implicated in the early events of imprinted X-inactivation (Mak et al., 2002; Wang et al., 2001b), which may be a temporally regulated event (Wutz and Jaenisch, 2000). Ezh2 and Eed are part of a single multimeric complex that includes histone deacetylase 1 and 2 (Tie et al., 2001; van der Vlag and Otte, 1999).

Ezh2 has a conserved SET (suppressor of variegation, enhancer of zeste and trithorax) domain (Laible et al., 1997), which is associated with histone methylation of lysine tails (Strahl and Allis, 2000). SET domains associated with Suv3-

9H1/2 (Rea et al., 2000), G9a (Tachibana et al., 2002), ESET (Yang et al., 2002), Set9/7 (Nishioka et al., 2002; Wang et al., 2001a) and PR-Set7 (Nishioka et al., 2002) all show histone methylation activities. Ezh2 also exhibits histone methylation activity in *Drosophila* and human cells (Cao et al., 2002; Czermin et al., 2002; Kuzmichev et al., 2002; Muller et al., 2002). Histone methylation can either repress or activate gene expression as it is present in both euchromatin and in heterochromatin. The two best-studied sites of histone H3 methylation are Lys9 (H3-K9), which is generally associated with repressive chromatin, and Lys4 (H3-K4), which is found in transcriptionally active DNA.

Little is known at present about the role of Ezh2 in very early mouse development. We first examined the role of maternally inherited Ezh2, and show that Ezh2 and Eed are involved in asymmetrical histone methylation of parental genomes in the early zygote. Depletion of maternal Ezh2 affects Ezh2-Eed colocalisation and histone methylation of the parental genomes, which results in a long-term effect on embryonic growth. At the blastocyst stage, we found that the Ezh2-Eed complex co-localises on the X chromosome in trophectoderm cells, where we detected H3-K27 methylation at the onset of X-inactivation; both the co-localisation of Eed and the histone methylation patterns were lost in the Ezh2 mutant blastocysts. We also detected a characteristic histone methylation pattern associated with the pluripotent epiblast cells in blastocysts, which was also abolished in the Ezh2 mutant embryos. Thus, Ezh2 is involved in early epigenetic events that regulate the histone methylation pattern in pluripotent epiblast cells and at the onset of differentiation of trophectoderm cells.

MATERIALS AND METHODS

Cryosectioning

Mouse ovaries were washed in cold PBS, mounted in Tissue Tek (Sakura), and frozen in liquid nitrogen prior to cutting 8 μm sections at –20˚C. Samples were fixed in 2% paraformaldehyde (PFA) for 10 minutes and stored in PBS. Immunostaining was performed as described below.

Genotyping of mice

Mice were genotyped by PCR or by standard Southern blot analysis with a 1 kb probe 1 on genomic tail tip DNA to identify wild type, targeted and deleted *Ezh2* alleles as described (Su et al., 2003)

Embryo collection and activation

Embryos were obtained from superovulated B6CBAF1 female mice as described (Hogan et al., 1994). Fertilised or unfertilised oocytes were collected in PB1 medium containing 300 μg/ml hyaluronidase and incubated for a few minutes to allow the cumulus cells to be shed. Pre-implantation embryos at other stages were usually collected by flushing the oviducts and uteri. Oocytes and pre-implantation embryos were cultured in T6/BSA under mineral oil at 37°C with 5% CO_2. Parthenogenetic embryos were obtained following incubation in 7% alcohol for 4.5 minutes (Cuthbertson, 1983) followed by incubation with Cytochalasin B for 4 hours to create diploid embryos.

Immunofluorescence and chromosome paint

Embryos were fixed in 4% PFA for 15 minutes and washed three times with PBS and permeabilised in AB-buffer (1% Triton-X100, 0.2% SDS, 10 mg/ml BSA in PBS) for 30 minutes. They were then incubated in primary antibody diluted in AB-buffer overnight at 4°C, followed by three AB-buffer washes of 10 minutes each and incubation in secondary antibodies (Alexa 564, Alexa 488, Molecular probes) for 1-2 hours in AB-buffer at room temperature, followed by AB-buffer washes as before and one wash in PBS. Finally the embryos were incubated in 0.1 mg/ml RNase A (Roche) in PBS at 37°C for 30 minutes and mounted on slides in Vectashield (Vector Laboratories) containing propidium iodide.

Primary embryonic fibroblasts (PEFs) were allowed to settle down on poly-L-lysine (Sigma)-coated slides after trypsination. Cells were rinsed in PBS and fixed for 15 minutes in 4% PFA in PBS at room temperature, followed by the protocol described above. X chromosome painting (Cambio) was performed as described in the manufacture's manual. Prior to in-situ hybridisation, embryos were treated as described (Costanzi and Pehrson, 1998) and immunofluorescence performed as described above. Immunofluorescence was visualised on a BioRad Radiance 2000 confocal microscope.

The following antibodies and dilutions were used: Ezh2 (A. Otte, 1:150), Eed (A. Otte, 1:100), HDAC1 (New England Biolabs, 1:100), H3-me_2-K4 (Upstate, 1:500), H3-me_2-K9 (Upstate, 1:500), H3-4x-me_2-K9 (T. Jenuwein, 1:250), H3-me_3-K9 (abcam, 1:150), H3-me_1-K27 (abcam, 1:150), H3-me_2-K27 (abcam, 1:150). Characterisation of H3-me_3-K9, H3-me_1-K27 and H3-me_2-K27 are published elsewhere (http://www.abcam.com); H3-me_3-K27 (T.J., unpublished). Antibodies were tested for their specificity in peptide competition assays (see supplementary Figures S1-S3 at http://dev.biologists.org/supplemental/).

Retroviral infection

Retrovirus was produced in Phoenix cells (gift from the Nolan laboratory) as described (Jackson-Grusby et al., 2001) and cells transfected with pMXpuro-CRE or pMXpuro-GFP using MBS KIT (Stratagene) as described in the manual. 72 hours after transfection, retrovirus containing supernatant was collected as described in pVPack vectors instruction manual (Stratagene) and PEFs from 12.5 dpc embryos infected with undiluted supernatant containing 4 μg/ml polyprene instead of 10 mg/ml DEAE-Dextran.

Immunoprecipitation

ES cells (from 129aa/129aa mice) were cultured on feeder layers until 80% confluency in LIF (1000 U/ml, ESGRO, Life Technologies) supplemented standard growth medium, washed twice in PBS and spun down at 1300 ***g***. The cell pellet from five 15 cm dishes was lysed in low-salt IPH buffer (50 mM Tris, pH 8.5; 100 mM NaCl; 0.5% NP40), vortexed and incubated on ice for 10 minutes. The lysate was spun down at 15,000 ***g*** at 4°C for 30 minutes and the supernatant incubated with Ezh2 antibodies or no antibodies (mock) at 4°C for 2 hours before adding washed sepharose G and A beads (1:1) (Pharmacia) and overnight incubation at 4°C. Beads were washed three times with low-salt IPH and subjected to methyltransferase assay.

Methyltransferase assays

For methyltransferase assays, the immunoprecipitated proteins or the mock precipitation were incubated with 10 μg of H3 peptides (H3 1-16: ARTKQTARKSTGGKAPGGC and H3 24-32 AARKSAPATGGC, methylated on lysines as indicated) together with 0.5 μCi of S-adenosyl-L-(methyl-3H) methionine (NEN) in methyltransferase buffer (final concentration: 50 mM NaCl, 25 mM TrisHCl pH. 8.8) for 1 hour at 30°C. Then 1 ml of binding buffer (20 mM TrisHCl pH 8.0, 5 mM EDTA pH 8.0) was added to the supernatant and the peptide was coupled to 25 μl of SulfLink beads (Pierce) for 1 hour. The beads were washed three times and the radioactivity counted by liquid scintillation.

Western blotting

Supernatant (5 μl) and IP-beads (5 μl) were boiled in SDS loading buffer for 10 minutes. Proteins were separated on 9% polyacrylamide

gels, blotted onto Immobilon-P membranes (Millipore), and probed for Ezh2 (1:1000), Eed (1:1000) or HDAC1 (1:500) according to standard protocols. Primary antibodies were detected with anti-mouse-HRP or anti-rabbit HRP (Amersham) followed by ECL detection (NEN Life Sciences).

RESULTS

The asymmetric localisation of maternally inherited Ezh2 and Eed in the zygote: effect of Ezh2 depletion

We have previously shown that Ezh2 has an essential role during early development and that *Ezh2* homozygous null mutation results in early lethality (O'Carroll et al., 2001). We now examine the role of Ezh2 from fertilisation through preimplantation development. The far-left panel of Fig. 1A summarises normal preimplantation development. Examining the distribution of Ezh2 from 0 to 10 hours post fertilisation (hpf), we found that Ezh2 is associated predominantly with the female genome between 0 and 3 hpf (Fig. 1B; left). Recruitment to the paternal pronucleus was delayed by several hours and becomes evident at about 6 hpf, increasing progressively thereafter (Fig. 1B). We then used a genetic approach to deplete the oocyte of maternally inherited Ezh2 before fertilisation (see below for details and Fig. 1A right panels). These zygotes were severely if not completely devoid of maternal Ezh2 (Fig.1C). As the oocytes were fertilised by wild-type sperm, we determined the time when the paternal allele commenced transcription, which turned out to be at about the four-cell stage (Fig. 1C).

We next asked if the maternal depletion of Ezh2 had any effect on the fate of maternally inherited Eed, which we also found to be asymmetrically localised at the maternal pronucleus at 0-3 hpf (Fig. 1D; left). In Ezh2 depleted zygotes, the localisation of Eed to the maternal pronucleus was also virtually absent (Fig. 1D, right). Thus, it appears that Eed localisation to parental pronuclei depends on its interacting partner, Ezh2.

Ezh2 depletion disrupts histone H3 methylation in the early zygote

Histone H3-tails can potentially be methylated at H3-K4, H3-K9 and H3-K27. As the Ezh2-Eed complex from ES cells showed histone methylation activity (see below), we examined control zygotes for histone methylation (see Materials and Methods; see supplementary Figures S1-S3 at http://dev.biologists.org/supplemental/). We found that mono-, di- and tri-H3-K27 methylation is strongly associated with the female pronucleus and the second polar body at the onset of development (Fig. 2A; left), while staining of the paternal pronucleus was observed several hours later, with a similar time course as shown for Ezh2 (Fig. 1B). The same situation was observed with di- and tri-H3-K9 specific antibodies. In mutant zygotes however, H3-K9 (not shown) and H3-K27 (Fig. 2A; right) was almost undetectable. When we tested H3-K4 methylation, the same asymmetry to the female pronucleus was observed but this was unchanged in Ezh2 mutant zygotes (not shown). We conclude that Ezh2 has a role in histone H3 methylation at least for H3-K27 and/or K9 methylation, either during oocyte development or in the zygote.

It is worth noting here that the protamine-histone exchange of the paternal genome occurs immediately after the entry of sperm into oocytes (Nonchev and Tsanev, 1990), and is therefore unlikely to explain the observed asymmetry. Furthermore, immunostainings of zygotes at this stage with pan-histone antibodies shows an equal distribution and access to antibodies in both pronuclei (Arney et al., 2002). Incidentally, we also noted an increased diameter of the zygotes and pronuclei in Ezh2 depleted zygotes compared with controls, which suggests that Ezh2 affects the size of the growing oocyte but the precise significance of this is unknown. All the nuclei of normal four-cell embryos are also positive for histone methylation at H3-K4, H3-K9 and H3-K27. Although the embryonic Ezh2 transcription commences at the 4-cell stage (see Fig. 1C), the histone methylation status was still substantially low at this stage (Fig. 2B), and did not reach levels comparable with controls until about the beginning of the 16-cell stage (Fig. 2B). Hence, there is a delay in the restoration of the normal epigenetic pattern in embryos that were depleted of maternally inherited Ezh2.

Developmental consequences of the depletion of maternally inherited Ezh2

To verify that Ezh2 is maternally inherited, we stained ovaries from wild-type female mice with Ezh2-specific antibodies. We found that Ezh2 is transcribed and stored as protein in the growing oocyte but not in the surrounding adult ovarian somatic tissues (Fig. 3A). To deplete the oocytes of this maternal inheritance, we used an *Ezh2* conditional allele in which exons 8-11 of the *Ezh2* gene were flanked by LoxP sites so that parts of the C-terminus, including the conserved SET domain, would be deleted in the presence of Cre-recombinase (Su et al., 2003). As mice inheriting two floxed alleles of *Ezh2* (*Ezh2*$^{F/F}$) were viable and without any detectable phenotypic consequences (Su et al., 2003), we crossed *Ezh2*$^{F/F}$ female mice with mice expressing Cre recombinase driven by the *Zp3* regulatory elements (ZP3-Cre), which is expressed exclusively in the growing oocyte prior to the completion of the first meiotic division (de Vries et al., 2000; Epifano et al., 1995). The *Ezh2*$^{F/F}$-*Zp3*-Cre females did show deletion of *Ezh2* (see Fig. 1C).

We next examined the consequences for development of the maternally depleted Ezh2 zygotes. We found that when Ezh2-depleted oocytes were fertilised by wild-type sperm, the *Ezh2*$^{DEL/F}$ progeny resulted in neonates with almost 40% less body weight, compared with the *Ezh2*$^{F/F}$ embryos with a similar genetic background and equivalent litter size (Fig. 3B). However, despite growth retardation, virtually all *Ezh2*$^{DEL/F}$ pups reached adulthood. This growth phenotype was present until about the weaning age of four weeks. After this time, these mice became indistinguishable from wild-type mice. They were also fertile.

However, unlike the *Ezh2*-null mice that show early embryonic lethality (O'Carroll et al., 2001), *Ezh2*$^{DEL/F}$ development proceeds to term, probably because the wild type paternal allele is activated at the four-cell stage and overcomes the early lethal phenotype observed in the homozygous mutant embryos. Indeed, we never obtained homozygous *Ezh2*$^{Del/Del}$ animals from any of our *Ezh2*$^{F/F}$ crosses, which is consistent with our previous studies (O'Carroll et al., 2001). By contrast, heterozygous *Ezh2*$^{+/-}$ animals with normal maternal Ezh2

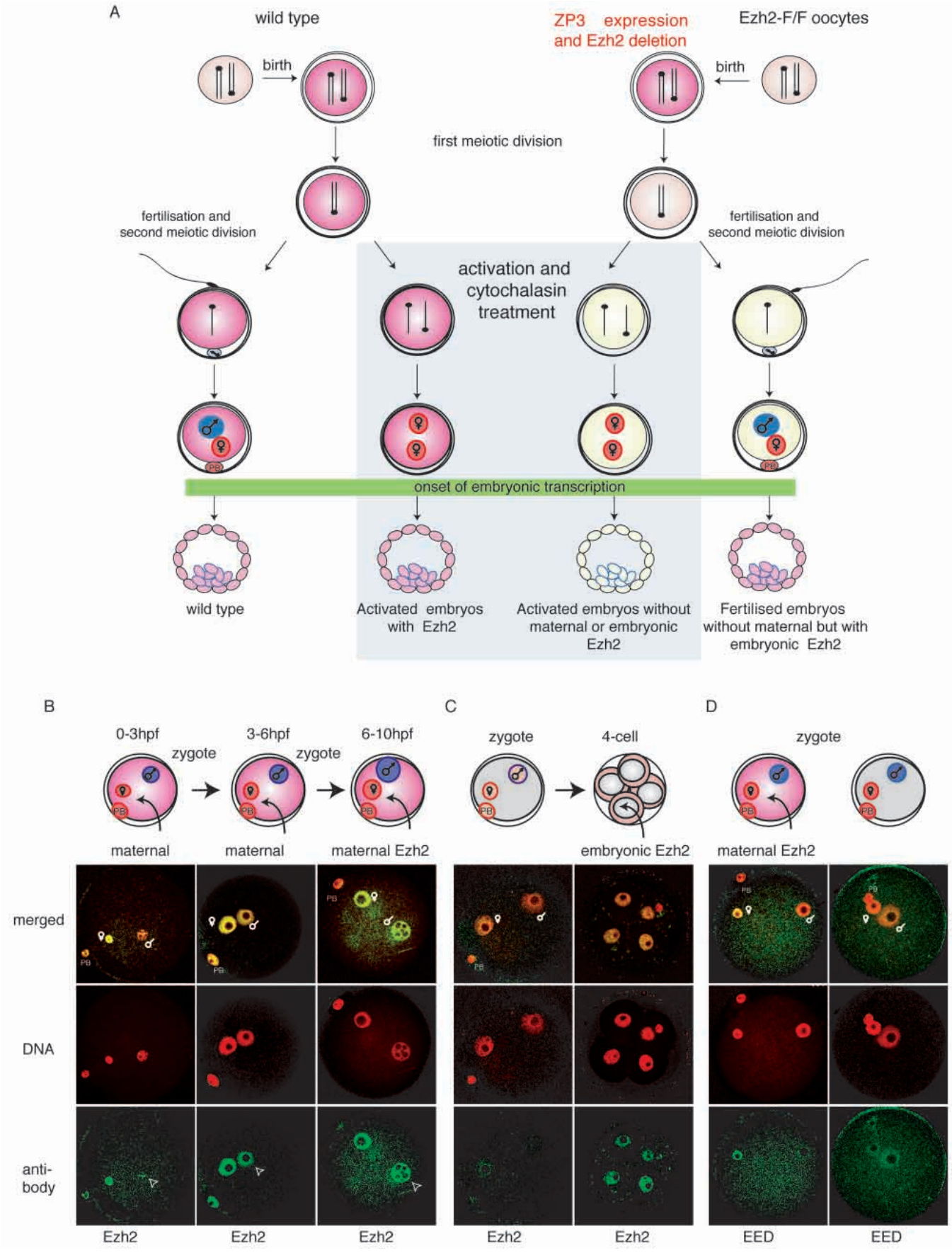
A
wild type
ZP3 expression and Ezh2 deletion
Ezh2-F/F oocytes
birth
birth
first meiotic division
fertilisation and second meiotic division
fertilisation and second meiotic division
activation and cytochalasin treatment
onset of embryonic transcription
wild type
Activated embryos with Ezh2
Activated embryos without maternal or embryonic Ezh2
Fertilised embryos without maternal but with embryonic Ezh2
B
0-3hpf
zygote
3-6hpf
zygote
6-10hpf
maternal
maternal
maternal Ezh2
C
zygote
4-cell
embryonic Ezh2
D
zygote
maternal Ezh2
merged
DNA
anti-body
Ezh2
Ezh2
Ezh2
Ezh2
Ezh2
EED
EED

Fig. 1. Asymmetric localisation of Ezh2/EED and the effect of Ezh2 depletion. (A) Schematic representation of oocyte maturation and preimplantation development (see left panels). The second meiotic division commences at fertilisation and the two parental genomes remain separate as pronuclei until the first cleavage division. Development can also be initiated by activation of oocytes without fertilisation, followed by the suppression of second polar body extrusion by cytochalasin B to generate diploid parthenogenetic embryos. To deplete the oocytes of maternal Ezh2, transgenic mice with the *Ezh2* conditional alleles, $Ezh2^{F/F}$, were crossed with ZP3 Cre recombinase transgenic animals to delete the $Ezh2^{F/F}$ alleles specifically in the growing oocyte (see far right panel). *Zp3* is expressed prior to the completion of the first meiotic division. Embryos depleted of maternal Ezh2 (right panels) were compared with those lacking both the maternal and embryonic Ezh2 (shown in the panel adjacent to the far-right panel). (B) Schematic depiction of development of zygotes at 0-3, 3-6 and 6-10 hours post fertilisation (hpf) (top line), with the corresponding immunostaining shown immediately below them. The haploid pronuclei inherited from the sperm and the oocyte can be distinguished morphologically (Hogan et al., 1994). Male and female pronuclei, and the second polar body (PB) are marked. All images in green show antibody staining, red shows DNA staining and yellow shows merged images. Ezh2 is first associated preferentially with the female pronucleus and the PB at 0-3 hpf. At ~3-6 hpf, Ezh2 can also be detected in the paternal pronucleus, and by 6-10 hpf, both male and female pronuclei show Ezh2 (white arrow heads). (C) Depicts a zygote depleted of maternally inherited Ezh2. Oocytes depleted of maternally inherited Ezh2 and fertilised by wild-type sperm show Ezh2 by immunostaining at the four-cell stage, indicating initiation of embryonic transcription of *Ezh2*. Note that the pronuclei in Ezh2 depleted zygotes appear to be slightly larger and less compact than in controls shown in 1B. (D) Eed is also asymmetrically localised to the female pronucleus (right panels). However, in Ezh2-depleted zygotes, asymmetric Eed localisation to the female pronucleus is highly reduced to virtually absent. Thus, asymmetrical localisation of Eed is apparently dependent on the maternal inheritance of Ezh2.

showed no detectable phenotype, which demonstrates that the maternal Ezh2 is necessary for normal development.

Our attempts to delete the paternal $Ezh2^{F/F}$ allele using the sperm-specific Cre line, *Sycp1* (Vidal et al., 1998) were unsuccessful. Therefore, we cannot rule out a function for Ezh2 during spermatogenesis or test the effect of the paternally inherited Ezh2 null allele. The phenotypic consequences of various genotypes with respect to *Ezh2* are summarised in Fig. 3C.

The role of Ezh2 during preimplantation development to the blastocyst stage

During development of preimplantation embryos to the blastocyst stage from a totipotent zygote, there is differentiation of trophectoderm cells and development of the inner cell mass (ICM) with pluripotent epiblast cells. Differentiation of trophectoderm (TE) is associated with the initiation of paternal X chromosome inactivation. We therefore went on to examine how the loss of Ezh2 affects these key epigenetic events.

The influence of Ezh2 on X-inactivation

To examine the role of Ezh2 during preimplantation development, we generated embryos depleted of both maternally inherited product and embryonic transcription (see Fig. 1C). To do so, we used activated oocytes (Barton et al., 2001; Hogan et al., 1994), thus avoiding the necessity for fertilisation and therefore the inheritance of a wild-type Ezh2 allele from sperm. Diploid parthenogenetic embryos (see Fig. 1A) have been studied extensively and shown to develop appropriately at least up to the blastocyst stage (Cuthbertson, 1983). Furthermore, although it is the paternal X chromosome that is preferentially inactivated in the trophectoderm in fertilised blastocysts (imprinted X inactivation), one of the two maternal X chromosomes in parthenogenetic embryos is selected to undergo inactivation in all embryos (Kay et al., 1994), which is reminiscent of the normal 'counting' mechanism involved in random X inactivation in the embryo proper of normal fertilised embryos, indicating that some of the mechanisms involved in X-inactivation are conserved in random and imprinted X inactivation.

To determine if there was a marked effect on development on embryos completely devoid of Ezh2, we compared parthenogenetic embryos from normal oocytes (henceforth called $PG^{+/+}$), with parthenogenetic embryos from Ezh2-deficient oocytes (henceforth called $PG^{-/-}$). $PG^{+/+}$ embryos, like fertilised embryos, will possess both the maternally inherited Ezh2, and the products of embryonic transcription, albeit from two maternal alleles. We found that both $PG^{+/+}$ and $PG^{-/-}$ developed to the blastocysts stage in vitro at about the same rate (not shown).

We then went on to examine the distribution of Ezh2 and Eed in trophectoderm cells, where they co-localise at the paternal X chromosome that undergoes X-inactivation (Mak et al., 2002). We found that ~50% of normally fertilised embryos from wild type animals (presumptive XX) showed this pattern (not shown). More importantly, all of the $PG^{+/+}$ blastocysts, which have two maternal X chromosomes, showed a similar co-localisation of Ezh2 and Eed to one of the two X chromosomes (Fig. 4A,B,D). This Ezh2-Eed co-localisation with the X_i was confirmed by Eed staining which always overlapped with the strongest macro-H2A signal, a histone variant, which is highly enriched on the X_i in trophectoderm (Costanzi and Pehrson, 1998) (Fig. 4E).

When we examined the consequences of Ezh2 depletion in $PG^{-/-}$ blastocysts we did not observe Ezh2 staining (not shown). More importantly, in the absence of Ezh2, we also did not detect the characteristic signal for Eed as seen at the X_i in $PG^{+/+}$ blastocysts (Fig. 4C). This observation clearly shows that co-localisation of Eed to the X_i is dependent on Ezh2. Incidentally, we also consistently detected higher overall staining of Eed in a small number of cells close to the ICM in both $PG^{+/+}$ and $PG^{-/-}$ blastocysts (Fig. 4B,C) but the nature of these cells has yet to be determined.

Ezh2-dependent histone methylation in trophectoderm cells

Next, we examined changes in histone methylation patterns at the blastocyst stage, and found no detectable differences when comparing $PG^{+/+}$ and blastocysts resulting from normal fertilisation. Both sets of blastocysts are referred to as control and compared with $PG^{-/-}$ blastocysts.

Immunostainings with an antibody raised against H3-me_3-K9 peptides showed brightly stained foci in controls (Fig. 5A, upper panel), which was similar to the pattern observed with the 'branched-K9' antibody, which recognises higher-order H3-K9 methylated chromatin (Maison et al., 2002). The

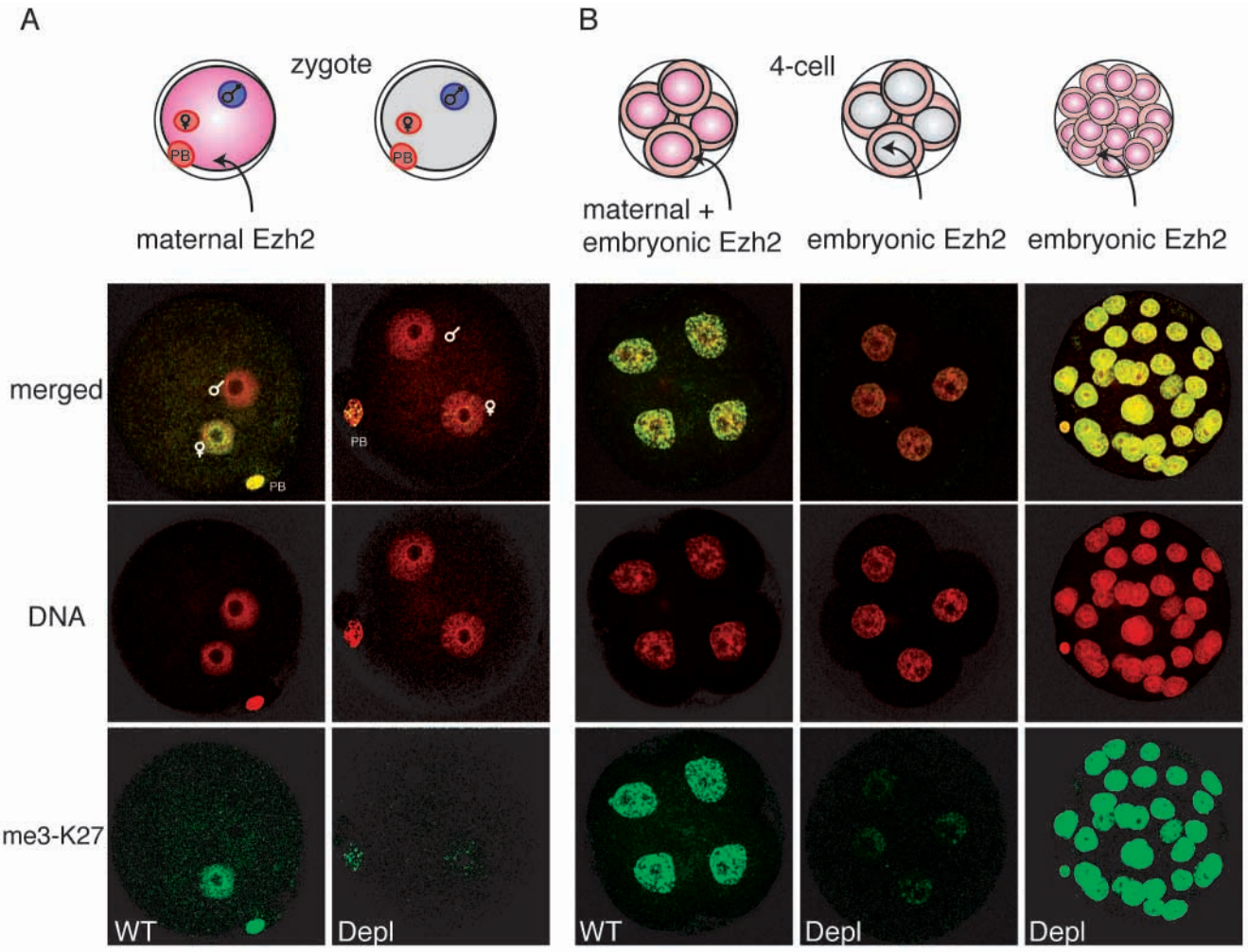

Fig. 2. Ezh2 depletion disrupts histone H3 methylation in zygotes and early embryos. (A) Wild-type zygotes at 0-3 hpf show histone H3-me$_3$-K27 methylation of the maternal pronucleus and of the PB. In the Ezh2-depleted zygote, H3-K27 methylation is markedly reduced (right panels). The H3-K9 shows a similar staining to H3-K27 but H3-K4 methylation is unchanged in Ezh2 depleted embryos (not shown). (B) A four-cell embryo with equal staining of all nuclei for H3-K27. In embryos depleted of maternally inherited Ezh2 (middle panel), the H3-27 is substantially less than in wild-type embryos (left panel). The H3-K27 levels are restored in these embryos at ~16- to 32-cell stage (far right panel). Bottom row, green shows antibody staining; middle row, DNA staining in red (propidium iodide); top row, merged images.

intensity and number of H3-me$_3$-K9 foci in PG$^{-/-}$ blastocysts were greatly diminished, especially in the TE cells (Fig. 5A; far-right picture). A more striking staining pattern was observed with H3-me$_2$-K27 antibodies, which in controls showed a strong overall staining of the ICM while TE cells showed a particularly intense staining concentrated in one spot per nucleus, similar to the staining pattern we observed for Ezh2 and Eed at this stage of development (Fig. 5B). This H3-me$_2$-K27staining also co-localises to one DNA dense region in trophoblast cells. Examining PG$^{-/-}$ blastocysts we found that the accumulation of H3-me$_2$-K27 in trophectoderm cells was completely lost (Fig. 5B, far-right). We observed identical staining patterns in controls with a me$_3$-K27 specific antibody (Fig. 5C). By contrast, we did not observe any obvious differences in staining pattern or intensity with the H3-me$_2$-K9-specific antibody when we compared PG$^{-/-}$ blastocysts with control embryos (see supplementary Figures S1-S3 at http://dev.biologists.org/supplemental/). These results indicate that the X_i is associated with H3-K27 methylation and that Ezh2, either directly or indirectly, mediates this methylation. Furthermore, in control embryos, H3-me$_3$-K27 co-localises with Eed, the interacting partner of Ezh2 (Fig. 5C). This H3-K27 methylation is associated with one X chromosome as shown by immunostaining in combination with X chromosome-specific fluorescence immunohybridisation in TE cells (Fig. 5D). As H3-K27 methylation co-localises with Eed and Ezh2 in TE cells, we can conclude that the X_i is associated with H3-K27 methylation at the onset of X-inactivation. Again, we observed a few cells in the ICM that were positive for H3-me$_2$-K27 and H3-me$_3$-K27, which were largely unaffected in PG$^{-/-}$ blastocysts.

As described recently, histone H3-K9 methylation is also a characteristic of the X_i (Boggs et al., 2002; Heard et al., 2001). However, when we double-stained controls with H3-me$_3$-K9 or branched H3-K9 (not shown) and Eed, we did not observe co-localisation of Eed and H3-K9 methylation (Fig. 5E). We

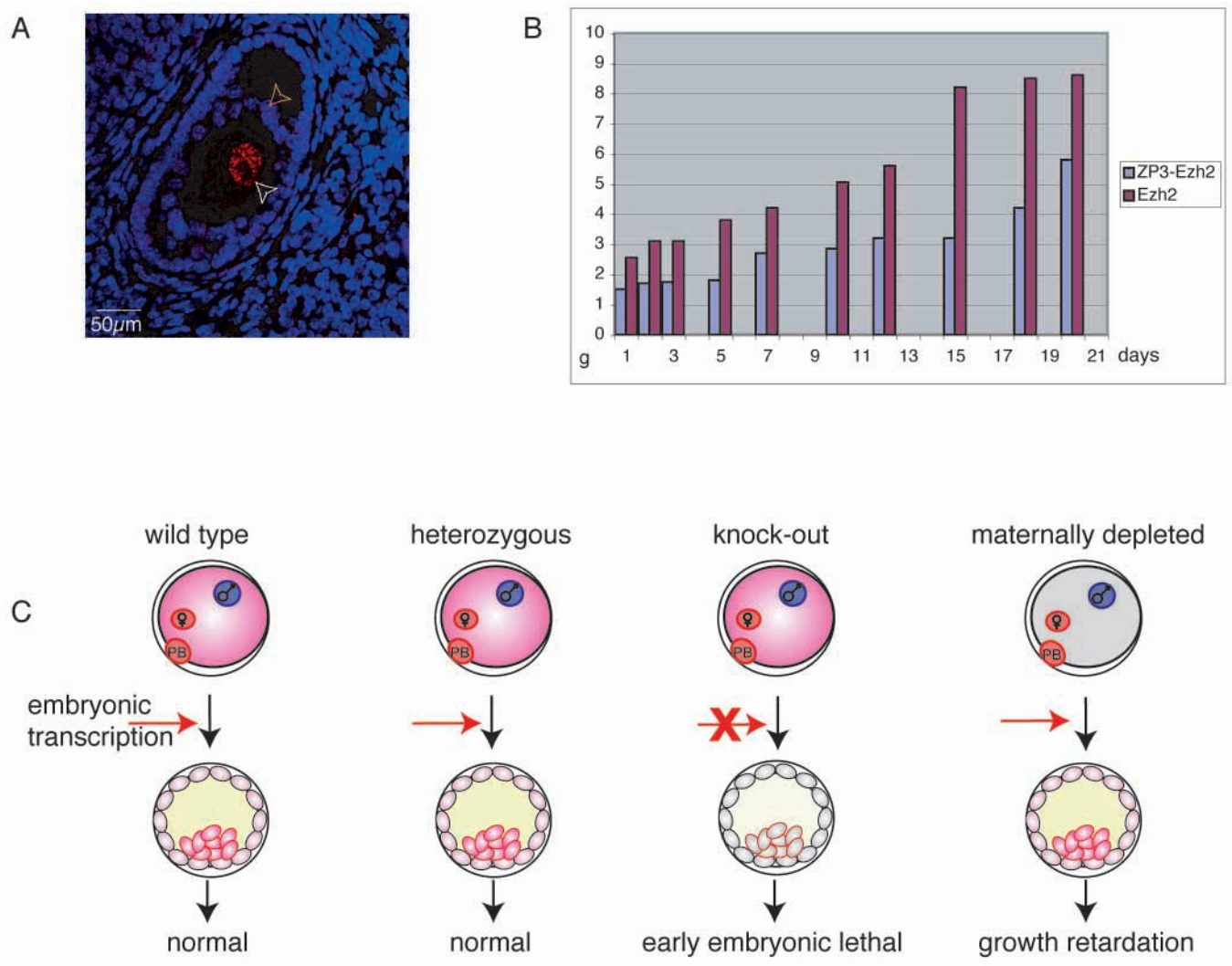

Fig. 3. (A) Cryosection of a wild-type ovary. The ovary is stained with anti-Ezh2 (red; white arrow head) but not the surrounding somatic cells and follicle cells (orange arrowhead). (B) The effect of depletion of maternally inherited Ezh2 results in growth retardation even though *Ezh2* transcription is restored at about the four-cell stage from the paternal allele (Fig. 1C), followed by a delayed restoration of normal H3-K27 by the 16-cell stage (Fig. 2B). The graph shows the average wet weight in grams of pups from Ezh2-depleted oocytes (blue bars) compared with pups with normal Ezh2 levels (red bars). (C) A summary of phenotypes with different mutations of *Ezh2*. Normal maternal inheritance of Ezh2 and one normal *Ezh2* allele is necessary for normal development [based on O'Carroll et al. (O'Carroll et al., 2001) and this study]. Mice from a conventional knockout approach die early during embryogenesis, despite maternal supply of Ezh2, indicating that the embryonic Ezh2 transcript is essential for development. Mice without maternal Ezh2 supply but embryonic transcription are viable and fertile, but display a severe growth retardation until about the weaning age of 4 weeks.

observed H3-me$_3$-K9 and branched H3-K9 staining only on the pericentric heterochromatin at this stage of development (Fig. 5F, left). Only occasionally at advanced blastocyst stages, we observed a few cells that showed co-localisation (not shown). One possible explanation is that the transient recruitment of Ezh2-Eed occurs before H3-K9 methylation on X_i because at later stages of development (9.5 dpc embryos) when Eed-Ezh2 no longer localise to the X_i, we observed H3-me$_3$-K9 and branched H3-K9/27 staining on the pericentric heterochromatin and on one entire chromosome, the presumptive the X_i (Fig. 5F, middle). We therefore suggest that the future X_i is not yet H3-K9 hypermethylated when Ezh2 and Eed are recruited. By contrast, when we stained controls with H3-me$_2$-K27 or me$_3$-K27, we observed one chromosome associated with H3-K27 methylation at the blastocyst stage (Fig. 5F, right). We therefore suggest that the future X_i is also highly methylated at H3-K27 and that this methylation occurs at the time when Eed-Ezh2 localises to the X_i and before the X_i becomes H3-K9 hypermethylated.

Ezh2 and histone methylation patterns in the ICM

With the H3-K27 antibodies (me$_1$-K27, me$_2$- K27, me$_3$-K27), we obtained a very intense staining in the ICM of controls, whereas the trophectoderm cells showed only a weak overall staining except for the X chromosome (Fig. 5B,C; Fig. 6A; see supplementary Figures S1-S3 at http://dev.biologists.org/supplemental/). This striking difference in histone methylation staining shows that there is an epigenetic difference between

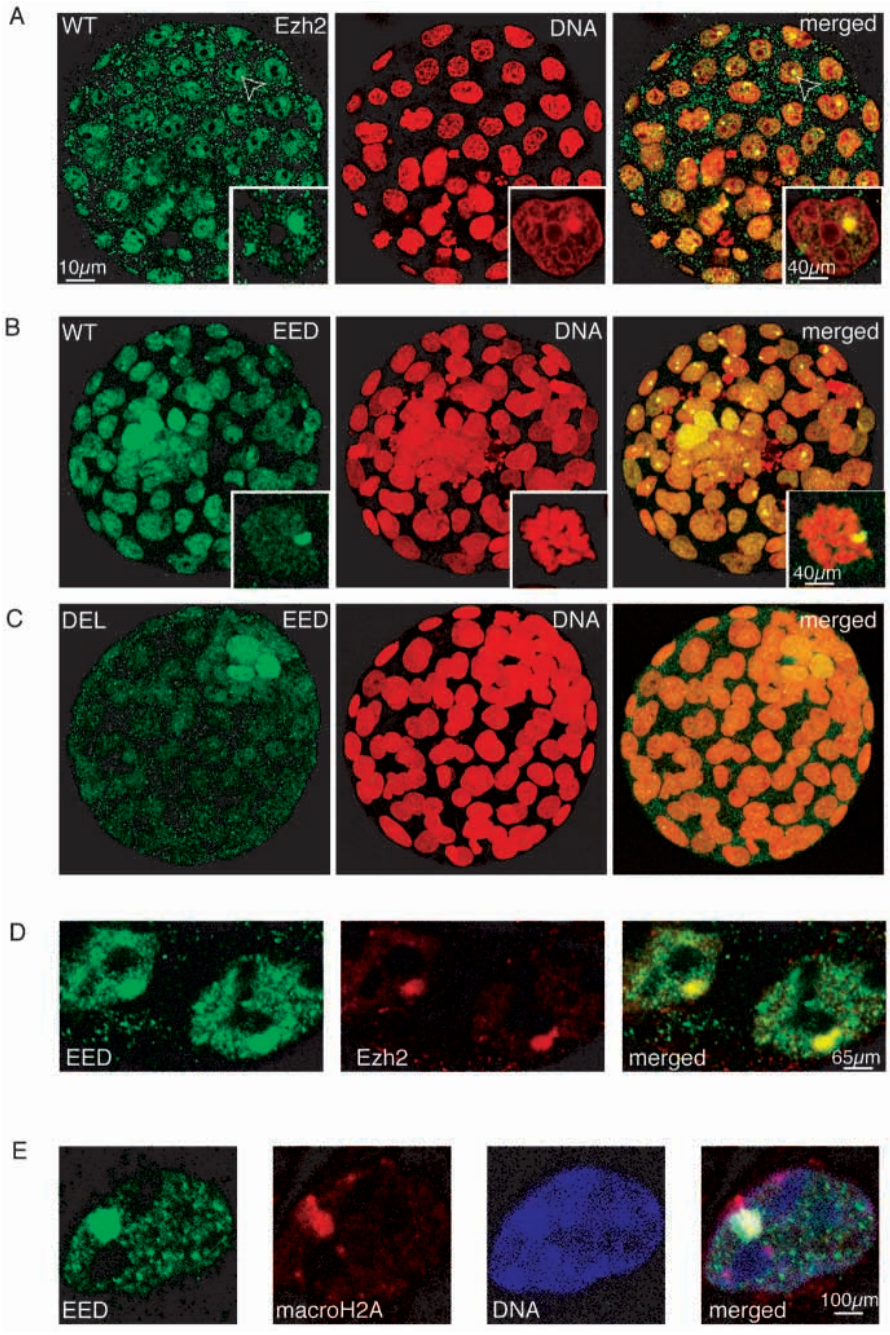

Fig. 4. Ezh2 and Eed co-localise at the X_i at the blastocyst stage. (A) Ezh2 distribution at the blastocyst stage of controls (fertilised or $PG^{+/+}$). In about 50% of blastocysts from fertilised oocytes, Ezh2 protein (green) is detected as a spot within the nucleus of TE cells (white arrowhead). The inset shows a higher magnification of a TE cell in a $PG^{+/+}$ blastocyst. The accumulation of Ezh2-Eed co-localises with a DNA dense region, presumably the inactivated X chromosome. As expected, $PG^{-/-}$ blastocysts do not show Ezh2 staining above background (not shown). (B) Eed distribution in $PG^{+/+}$ blastocysts, which is similar to the staining for Ezh2 shown in A. The inset shows that Eed stays associated with one chromosome (DNA in red) during M-phase at the blastocyst stage, presumably the inactive X chromosome. (C) Eed staining in $PG^{-/-}$ blastocysts shows none of the localisation of Eed seen in $PG^{+/+}$ blastocysts shown in B. (D) Ezh2 (red) and Eed (green) co-localise in trophectoderm cells at the blastocyst stage, presumably at the inactivated X chromosome. The image shows immunostaining of two TE cells from $PG^{+/+}$ blastocysts. (E) Eed co-localises with macro-H2A in trophectoderm cells at the blastocyst stage in $PG^{+/+}$ blastocysts. Macro-H2A is highly enriched on the X_i (Costanzi and Pehrson, 1998), indicating that Ezh2 and Eed are also associated with the X_i.

cells of the pluripotent ICM and differentiated TE cells.

To confirm that these differences are associated with the pluripotent epiblast cells within the ICM, we immunostained fertilised blastocysts from a transgenic line that expresses *Oct4-GFP* in pluripotent cells (Hajkova et al., 2002; Nichols et al., 1998). Indeed, we found that cells from blastocysts, which were positive for GFP, displayed a strong overall signal for H3-me_3-K27 methylation (Fig. 6A). We concluded that the characteristic H3-me_3-K27 pattern is associated with the pluripotent cells of the ICM. The H3-me_3-K27 staining pattern and intensity were similar to those we have detected at the morula stage (Fig. 6B), suggesting that this is a hallmark of pluripotent cells during early development.

To test whether Ezh2 is also necessary in cells from later embryos, we obtained primary embryonic fibroblasts (PEFs) with a null and floxed allele for *Ezh2* and infected them with Cre or GFP expression retroviral supernatant (Jackson-Grusby et al., 2001). When the floxed allele was excised by Cre to generate PEFs lacking Ezh2, we could not detect a significant effect on proliferation in these cells compared with the controls (see Fig. 6C), even though Ezh2 protein levels were highly reduced in Cre-infected cells as early as 3 days after infection (Fig. 6D). Thus, Ezh2 is essential for early developmental events and in pluripotent ES cells, but not in differentiated cells.

The Ezh2/Eed complex has histone methyltransferase activity for K9 and K27

Histone modifications as judged by antibody staining suggest that Ezh2 has histone methyltransferase activity (HMTase), particularly for K9 and K27, which is abolished in Ezh2 depleted embryos. To verify this observation, we assayed for HMTase activity in pluripotent murine ES cells. We immunoprecipitated Ezh2 from total ES cell extract and tested the antibody bound fraction for HMTase activity. Using differentially methylated peptides as substrates (Fig. 7A), we observed HMTase activity specifically for H3-K9 and for H3-K27, with the highest activity for H3-K27 (Fig. 7B). Furthermore, we confirmed by western blotting the presence of Ezh2, Eed and HDAC1 in the precipitated fraction (Fig. 7C). Our data strongly indicate that the

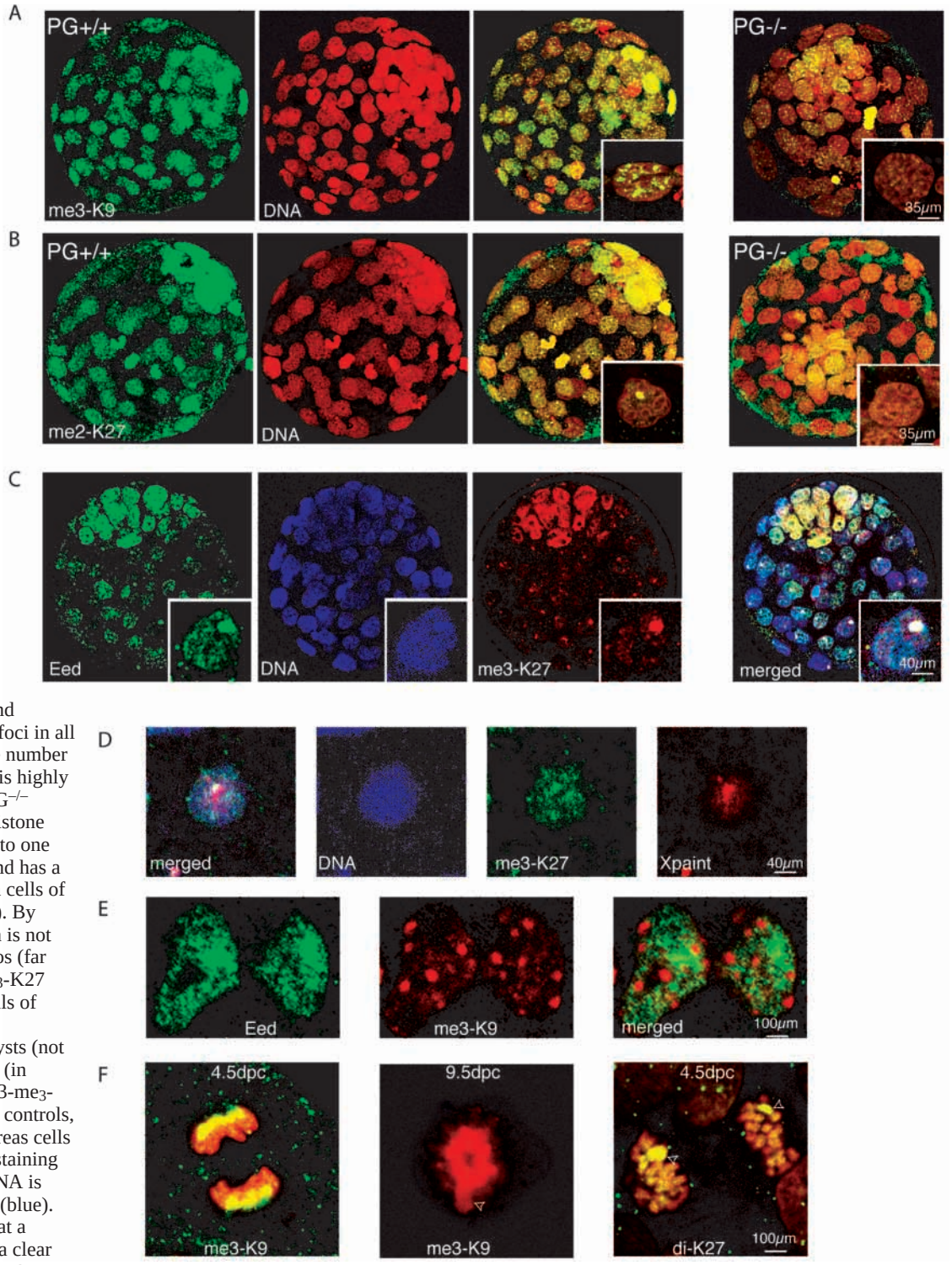

Fig. 5. Histone methylation patterns are disturbed in the absence of Ezh2. (A) Histone H3-me_3-K9 modification is present mainly in pericentric heterochromatic regions and can be detected as several foci in all cells of controls (left). The number and intensity of these foci is highly reduced in most cells of $PG^{-/-}$ embryos (far-right). (B) Histone H3-me_2-K27 accumulates to one region in cells of the TE and has a stronger overall staining in cells of the presumptive ICM (left). By contrast, this accumulation is not detectable in $PG^{-/-}$ embryos (far right). (C) Histone H3-me_3-K27 also accumulates in TE cells of control embryos, which is abolished in $PG^{-/-}$ blastocysts (not shown). Eed accumulation (in green) co-localises with H3-me_3-K27 (in red) in TE cells of controls, presumably at the X_i, whereas cells of the ICM show a bright staining throughout the nucleus. DNA is counterstained with Toto3 (blue). The insets show a TE cell at a higher magnification with a clear co-localisation of Eed and H3-me_3-K27. (D) Fluorescence in-situ hybridisation (FISH) using a mouse X chromosome specific paint (red) combined with immunofluorescence shows that H3-me_3-K27 (green) is associated with one X chromosome in a TE cell at the blastocyst stage. DNA is counterstained with Toto3 (blue). Metaphase chromosomes stained for H3-me_3-K9 and H3-me_1-K27 stained very brightly in control embryos and in $PG^{-/-}$, owing to a higher accessibility of antibodies to metaphase chromosomes in early embryos. (E) Eed (green) accumulation at the X_i does not co-localise with H3-me_3-K9 (red) in TE cells of controls. (F) Metaphase chromosomes in control embryos stain brightly for H3-me_3-K9 in the pericentric heterochromatin (left, yellow staining). At later stages of development (9.5dpc), when Ezh2/Eed do not co-localise to the X_i any more (not shown), H3-me_3-K9 specific antibodies stain one entire chromosome (white arrow head) in addition to pericentric heterochromatin in female embryos (middle). By contrast, me_2- (and me_3-) K27 is highly associated with one chromosome in control embryos at the blastocyst stage (right, white arrowheads), as well as in 50% of wild-type embryos at the blastocyst stage (not shown). D-F show TE cells in interphase (D,E) or metaphase (F) of normal fertilised embryos.

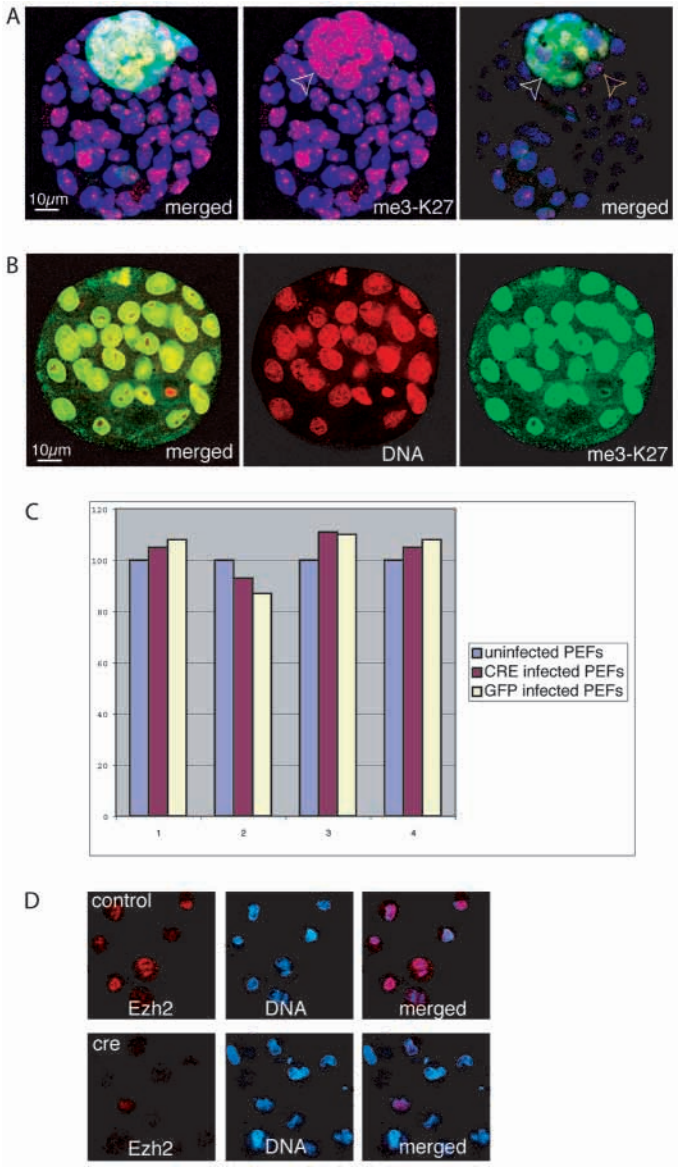

Fig. 6. The ICM with pluripotent epiblast cells shows a specific and characteristic histone methylation pattern that is distinct from the pattern seen in TE cells. (A) The ICM with pluripotent epiblast cells has high me_1-, me_2- and me_3-K27 methylation levels (pink, middle). These cells show expression of Oct4-GFP, which is a marker of pluripotent epiblast cells (green, right). This pattern of histone methylation differs from that in trophectoderm cells shown in Fig. 4. Cells that show clustering of di- and tri-K27 methylation on the X_i do not express Oct4-GFP (green), which is most obvious in single optical sections (right). The white arrowheads in the middle and right images indicate an *Oct4-GFP*-expressing cell in the ICM with high me_3-K27 levels. The orange arrowhead indicates an Oct4-GFP negative cell that is undergoing X-inactivation. (B) The high levels of H3-K27 methylation of the ICM is similar to the staining at earlier stages of development, when all cells are pluripotent. The images show a late morula stage just prior to the blastocyst stage. (C) Deletion of *Ezh2* from primary embryonic fibroblasts (PEFs) show no detectable effects on growth. Growth of PEFs was monitored in uninfected, GFP-infected and Cre-infected cells after three (1), five (2), six plus one passages (3) and eight days (4) in culture after infection. (F) Immunostaining of control GFP (upper panel) and experimental Cre (lower panel)-infected PEFS. The Ezh2 protein level was already highly reduced three days after Cre infection (lower panel) compared with GFP-infected cells (upper panel) as shown by immunofluorescence (DNA in blue, Ezh2 in red).

Ezh2/Eed complex has an intrinsic H3-K9/K27 specific HMTase activity that is probably associated with Ezh2 that has the SET domain characteristic. Recent findings from *Drosophila* and human cells support our findings (Cao et al., 2002; Czermin et al., 2002; Kuzmichev et al., 2002; Muller et al., 2002).

DISCUSSION

We have demonstrated that Ezh2 has a critical role in early mouse development (see summary in Fig. 8). Depletion of maternal Ezh2 affects the preferential localisation of Eed to the maternal pronucleus in early zygotes, as well as the epigenetic asymmetry between parental genomes for histone H3-K27 and H3-K9 modifications. We have demonstrated that these early events in the zygote are important for development as the lack of maternal Ezh2 has long-term developmental consequences resulting in severe growth retardation of neonates. This phenotypic effect occurs despite restoration of *Ezh2* transcription from the paternal allele as early as the four-cell stage. We have also observed Ezh2-Eed-dependent epigenetic modifications in pluripotent epiblast and in trophectoderm cells, most prominently the X_i where Ezh2-Eed co-localise with H3-K27 modification. It is not possible to derive ES cells from Ezh2 null blastocysts (O'Carroll et al., 2001). The Ezh2 may therefore be crucial for the propagation of the pluripotent state and during the early stages of cell fate determination, which is consistent with the early embryonic lethality of $Ezh2^{-/-}$ embryos. By contrast, *Eed* mutant blastocysts give rise to ES cells and these mutant ES cells contribute to chimeric mice, indicating a fundamental difference in the importance of these proteins for pluripotent cells (Morin-Kensicki et al., 2001).

Ezh2, a regulator of the epigenetic asymmetry between parental genomes

Oocytes depleted of the maternal supply of Ezh2 show severe growth retardation, even when fertilised by wild-type sperm. As both male and female embryos show this phenotype, it is not linked to X-inactivation. *Ezh2* heterozygosity per se does not give this phenotype, thus excluding this as an Ezh2 dose-dependent phenotype. Apart from Ezh2-Eed, HP1beta, which binds to H3-K9 methylated histone tails, is also first recruited to the maternal pronucleus in the zygote (Arney et al., 2001). At this time, the paternal genome undergoes preferential, rapid and genome-wide DNA demethylation (Mayer et al., 2000; Oswald et al., 2000; Santos et al., 2002), and histone H4-K5 acetylation rises rapidly on the paternal genome (Adenot et al., 1997).

The purpose and importance of the epigenetic asymmetry between parental genomes has been considered in the context of genomic imprinting (Surani, 2001; Ferguson-Smith and Surani, 2001). It is thought that the oocyte cytoplasm has played a significant role in discriminating between parental

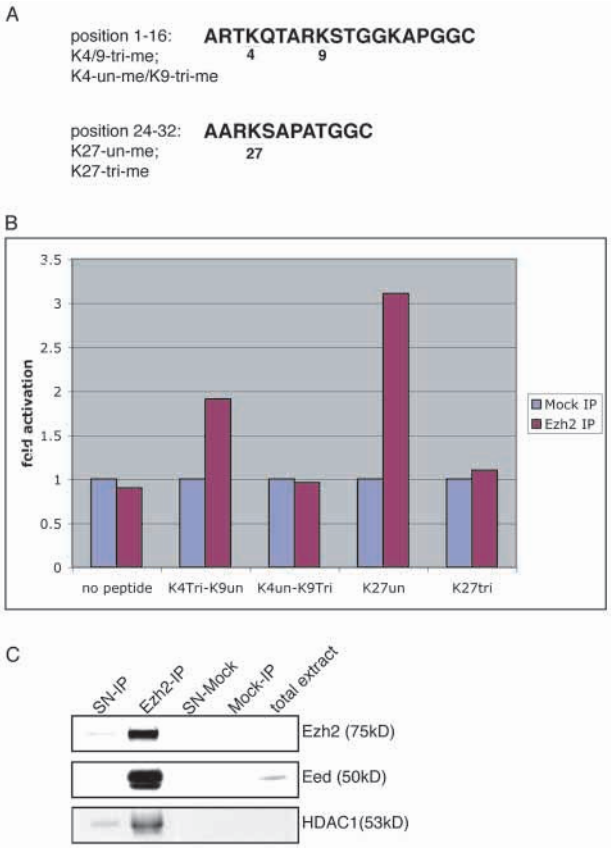

Fig. 7. Immunoprecipitation (IP) with Ezh2 antibodies shows histone methyltransferase (HMTase) activity for K9 and K27. (A) HMTase activity was tested on two different types of peptides with various combinations of lysine methylation. (B) HMTase assay of Ezh2 IP from ES cell extract on peptides as substrate. The immunoprecipitate showed highest HMTase activity for K27-unmethylated peptides and a lower activity for peptides, which were unmethylated at K9 but fully methylated at K4. (C) Western blot analysis of IP-bound beads and supernatant (SN) showed that the Ezh2 antibodies precipitate Ezh2 and that Eed and HDAC1 are bound to this complex.

genomes during evolution, for example in the selective elimination of paternal chromosomes in some lower organisms (Werren and Hatcher, 2000). The epigenetic differences between parental genomes in the mouse zygote are not observed in lower vertebrates and may have arisen according to the genomic conflict hypothesis that was proposed to explain genomic imprinting (Haig and Graham, 1991; Reik and Walter, 2001). In this context, disruption of imprinting in interspecific hybrids of the deermouse *Peromyscus maniculatus*, may be due to nuclear-cytoplasmic incompatibility (Vrana et al., 1998). As the neonates recover from the growth deficiency after weaning, it is possible that the absence of Ezh2 may affect the placenta. It has been shown, for example, that specific disruption of imprinting of *Igf2* in the placenta has a marked effect on foetal growth, which is subsequently restored in neonates after weaning (Constancia et al., 2002). We propose in the future to examine whether the absence of Ezh2 in oocytes has an effect on placental development, on physiological functions and on the status of imprinted genes.

Mammalian development is also marked by the early activation of the embryonic genome. Ezh2, Eed and other epigenetic modifiers may establish a new higher-order chromatin structure that may be important for this purpose (Fig. 8). As with DNA methylation, establishment, maintenance and heritability of histone methylation patterns may be distinct events requiring different modifiers. For example, HMTases, including G9a and Ezh2, are required early in development whereas others, such as Suv3-9H, have a more

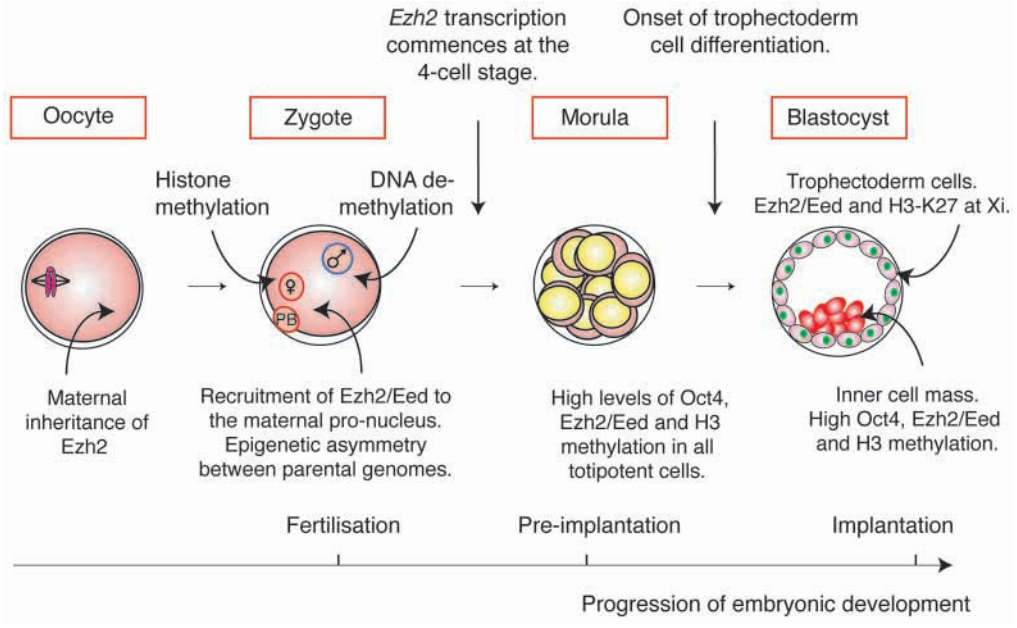

Fig. 8. Summary of histone H3 methylation events and the role of Ezh2 at the onset of mouse development. Shortly after fertilisation, Ezh2/Eed and H3 methylation are predominantly associated with the female pronucleus, and establish an epigenetic asymmetry between the two parental genomes. When this asymmetry is disturbed after depletion of the maternally inherited Ezh2, there is a long-term effect resulting in severe growth retardation of neonates even when the embryonic transcription occurs at the four-cell stage. The epigenetic asymmetry therefore has a significant effect on development and fetal growth. During cleavage stages, Ezh2/Eed and H3 methylation levels are high. At this stage, all cells are pluripotent. During differentiation of TE cells, there are significant changes in the subnuclear localisation and levels of Ezh2/Eed and H3 histone methylation. The pluripotent epiblast cells that continue to express *Oct4* retain a characteristic and a distinct histone methylation pattern consistent with the epigenetic plasticity of these cells.

subtle effect on early development (O'Carroll et al., 2001; Peters et al., 2001; Tachibana et al., 2002). The Ezh2-Eed complex contains HDAC1/2 as well as the intrinsic HMTase activity, which are two significant chromatin modifications that have the potential for establishing new gene expression patterns. There is continuing genome-wide DNA demethylation during preimplantation development, which reaches the lowest point at the blastocyst stage (Carlson et al., 1992; Howlett and Reik, 1991; Kafri et al., 1993; Monk et al., 1987). It is perhaps at this time that the Ezh2-Eed complex might play a crucial role in establishing a new epigenetic pattern in the epiblast and the trophectoderm. It is possible that the epigenetic patterns established by histone methylation may be followed by appropriate DNA methylation patterns, as seems to be the case in *Neurospora* (Tamaru and Selker, 2001) and possibly in *Arabidopsis* (Jackson et al., 2002).

The role of Ezh2-Eed in the initiation of X-inactivation in trophectoderm cells

We have shown that the Ezh2-Eed complex in blastocysts co-localises to the X_i, an event that is disrupted in the Ezh2 mutant embryos accompanied by the loss of H3-K27 methylation. The recruitment of the Ezh2-Eed complex to the X_i is restricted to early development only, but X-inactivation is stably propagated thereafter. We propose that the Ezh2-Eed complex has the enzymatic properties to establish an early mark for X-inactivation in the form of H3-K27 methylation prior to H3-K9 methylation. Once H3-K27 methylation is established, we suggest two alternative pathways for establishing stable X-inactivation. Either H3-K27 methylation recruits further factors or complexes with H3-K9 HMTase activity, or H3-K9 methylation on the X_i is also catalysed by Ezh2. In contrast to H3-K27 methylation, we do not see a strong co-localisation of Ezh2 and H3-K9 methylation. However, if we assume that H3-K9 methylation follows H3-K27 methylation at the blastocyst stage, the time window of co-localisation between Ezh2-Eed and H3-K9 could be very short.

As stated above, we have made similar observations in both $PG^{+/+}$ and normal blastocysts. Since $PG^{+/+}$ have two maternal X chromosomes, there would be a random choice of which chromosome undergoes inactivation, as suggested from previous studies (Iwasa, 1998). It is therefore also likely that the same mechanism involving Ezh2-Eed must operate during random inactivation in XX embryonic cells.

Ezh2 and pluripotency

Early mammalian development differs from that in other vertebrates because of the necessity to generate extra-embryonic trophectoderm cells, as well as the pluripotent epiblast cells, from which both the embryo proper and germ cells are derived. Oct4 is clearly essential for pluripotency (Rossant, 2001). It is noteworthy that the presence of Oct4 is always accompanied by the presence of Ezh2 and Eed, which is the case in the zygote, early blastomeres, epiblast and pluripotent stem cells. It is important to note a characteristic and distinct staining pattern for H3-K27/9 histone methylation in pluripotent epiblast cells compared with trophectoderm cells, which coincides with the expression of Oct4-GFP. We know that both Ezh2 and Oct4 are also highly expressed in pluripotent ES cells, and they are both crucial for the propagation of the pluripotent state; their levels decline after the onset of differentiation. Loss of function of either of these two genes results in the loss of these pluripotent cells (Nichols et al., 1998). The Ezh2-mediated H3-K27/K9 methylation in pluripotent epiblast cells is clearly affected in Ezh2 depleted blastocysts. These results strongly argue that Ezh2 is important for maintaining the epigenetic plasticity of pluripotent epiblast and of ES cells. It is also noteworthy that in both the zygote and in germ cells major epigenetic reprogramming events occur against a background of high Ezh2 and Oct4 (Hajkova et al., 2002; Lee et al., 2002). In summary, we have shown here that the early histone modifications in the zygote, the trophectoderm and in epiblast cells all depend on Ezh2. Thus, Ezh2 seems to mediate histone modifications in totipotent/pluripotent cells, and it may be crucial for early cell fate determination. Our study may, in the future, provide a link between histone modifications, epigenetic gene regulation by PcG genes and the establishment of epigenetic marks that are apparently crucial for early development and for pluripotency.

Very recent publications on Ezh2 support our findings and conclusions that the X_i is associated with H3-K27 methylation (Silva et al., 2003; Plath et al., 2003).

We are grateful to A. Otte for the gift of Ezh2 and Eed antibodies, W. N. de Vries and B. B. Knowles for the Zp3 Cre transgenic mice, and R. Jaenisch for the retroviral constructs. S.E. acknowledges support from the Boehringer Ingelheim Fonds. Work of R.S. is funded by an HFSP fellowship. Work in laboratory of the T.K. is funded by a CR UK grant. Work in the laboratory of M.A.S. is funded by the Wellcome Trust and BBSCR. The generation of mice carrying conditional *Ezh2* allele was conducted in the laboratory of Lymphocyte Signaling, Rockefeller University, New York and supported by the Irene Diamond Foundation.

REFERENCES

Abel, K. J., Brody, L. C., Valdes, J. M., Erdos, M. R., Mckinley, D. R., Castilla, L. H., Merajver, S. D., Couch, F. J., Friedman, L. S., Ostermeyer et al. (1996). Characterization of Ezh1, a human homolog of Drosophila enhancer of zeste near brca1. *Genomics* **37**, 161-171.

Adenot, P. G., Mercier, Y., Renard, J. P. and Thompson, E. M. (1997). Differential H4 acetylation of paternal and maternal chromatin precedes DNA replication and differential transcriptional activity in pronuclei of 1-cell mouse embryos. *Development* **124**, 4615-4625.

Arney, K. L., Bao, S., Bannister, A. J., Kouzarides, T. and Surani, M. A. (2002). Histone methylation defines epigenetic asymmetry in the mouse zygote. *Int. J. Dev. Biol.* **46**, 317-320.

Arney, K. L., Erhardt, S., Drewell, R. A. and Surani, M. A. (2001). Epigenetic reprogramming of the genome–from the germ line to the embryo and back again. *Int. J. Dev. Biol.* **45**, 533-540.

Barton, S. C., Arney, K. L., Shi, W., Niveleau, A., Fundele, R., Surani, M. A. and Haaf, T. (2001). Genome-wide methylation patterns in normal and uniparental early mouse embryos. *Hum. Mol. Genet.* **10**, 2983-2987.

Boggs, B. A., Cheung, P., Heard, E., Spector, D. L., Chinault, A. C. and Allis, C. D. (2002). Differentially methylated forms of histone H3 show unique association patterns with inactive human X chromosomes. *Nat. Genet.* **30**, 73-76.

Cao, R., Wang, L., Wang, H., Xia, L., Erdjument-Bromage, H., Tempst, P., Jones, R. S. and Zhang, Y. (2002). Role of histone H3 lysine 27 methylation in Polycomb-group silencing. *Science* **298**, 1039-1043.

Carlson, L. L., Page, A. W. and Bestor, T. H. (1992). Properties and localization of DNA methyltransferase in preimplantation mouse embryos: implications for genomic imprinting. *Genes Dev.* **6**, 2536-2541.

Chen, H. M., Rossier, C. and Antonarakis, S. E. (1996). Cloning of a human homolog of the Drosophila-enhancer-of-zeste gene (Ezh2) that maps to chromosome 21q22.2. *Genomics* **38**, 30-37.

Constancia, M., Hemberger, M., Hughes, J., Dean, W., Ferguson-Smith, A., Fundele, R., Stewart, F., Kelsey, G., Fowden, A., Sibley, C. and Reik,

W. (2002). Placental-specific IGF-II is a major modulator of placental and fetal growth. *Nature* **417**, 945-948.
Costanzi, C. and Pehrson, J. R. (1998). Histone macroH2A1 is concentrated in the inactive X chromosome of female mammals. *Nature* **393**, 599-601.
Cuthbertson, K. S. (1983). Parthenogenetic activation of mouse oocytes in vitro with ethanol and benzyl alcohol. *J. Exp. Zool.* **226**, 311-314.
Czermin, B., Melfi, R., McCabe, D., Seitz, V., Imhof, A. and Pirrotta, V. (2002). Drosophila Enhancer of Zeste/ESC complexes have a Histone H3 methyltransferase activity that marks chromosomal Polycomb sites. *Cell* **111**, 185-196.
de Vries, W. N., Binns, L. T., Fancher, K. S., Dean, J., Moore, R., Kemler, R. and Knowles, B. B. (2000). Expression of Cre recombinase in mouse oocytes: a means to study maternal effect genes. *Genesis* **26**, 110-112.
Epifano, O., Liang, L. F., Familari, M., Moos, M. C., Jr and Dean, J. (1995). Coordinate expression of the three zona pellucida genes during mouse oogenesis. *Development* **121**, 1947-1956.
Faust, C., Lawson, K. A., Schork, N. J., Thiel, B. and Magnuson, T. (1998). The Polycomb-group gene eed is required for normal morphogenetic movements during gastrulation in the mouse embryo. *Development* **125**, 4495-4506.
Ferguson-Smith, A. C. and Surani, M. A. (2001). Imprinting and the epigenetic asymmetry between parental genomes. *Science* **293**, 1086-1089.
Grossniklaus, U., Vielle-Calzada, J. P., Hoeppner, M. A. and Gagliano, W. B. (1998). Maternal control of embryogenesis by MEDEA, a polycomb group gene in Arabidopsis. *Science* **280**, 446-450.
Haig, D. and Graham, C. (1991). Genomic imprinting and the strange case of the insulin-like growth factor II receptor. *Cell* **64**, 1045-1046.
Hajkova, P., Erhardt, S., Lane, N., Haaf, T., El-Maarri, O., Reik, W., Walter, J. and Surani, M. (2002). Epigenetic reprogramming in mouse primordial germ cells. *Mech. Dev.* **117**, 15-23.
Heard, E., Rougeulle, C., Arnaud, D., Avner, P., Allis, C. D. and Spector, D. L. (2001). Methylation of histone H3 at Lys-9 is an early mark on the X chromosome during X inactivation. *Cell* **107**, 727-738.
Hobert, O., Sures, I., Ciossek, T., Fuchs, M. and Ullrich, A. (1996). Isolation and developmental expression analysis of Enx-1, a novel mouse Polycomb group gene. *Mech. Dev.* **55**, 171-184.
Hogan, B., Beddington, R., Constantini, F. and Lacy, E. (1994). *Manipualting The Mouse Embryo: A Laboratory Manual*. Cold Spring Harbor: Cold Spring Harbor Laboratory Press.
Howlett, S. K. and Reik, W. (1991). Methylation levels of maternal and paternal genomes during preimplantation development. *Development* **113**, 119-127.
Iwasa, Y. (1998). The conflict theory of genomic imprinting: how much can be explained? *Curr. Top. Dev. Biol.* **40**, 255-293.
Jackson, J. P., Lindroth, A. M., Cao, X. and Jacobsen, S. E. (2002). Control of CpNpG DNA methylation by the KRYPTONITE histone H3 methyltransferase. *Nature* **416**, 556-560.
Jackson-Grusby, L., Beard, C., Possemato, R., Tudor, M., Fambrough, D., Csankovszki, G., Dausman, J., Lee, P., Wilson, C., Lander, E. and Jaenisch, R. (2001). Loss of genomic methylation causes p53-dependent apoptosis and epigenetic deregulation. *Nat. Genet.* **27**, 31-39.
Kafri, T., Gao, X. and Razin, A. (1993). Mechanistic aspects of genome-wide demethylation in the preimplantation mouse embryo. *Proc. Natl. Acad. Sci. USA* **90**, 10558-10562.
Kay, G. F., Barton, S. C., Surani, M. A. and Rastan, S. (1994). Imprinting and chromosome counting mechanisms determine Xist expression in early mouse development. *Cell* **77**, 639-650.
Kuzmichev, A., Nishioka, K., Erdjument-Bromage, H., Tempst, P. and Reinberg, D. (2002). Histone methyltransferase activity associated with a human multiprotein complex containing the Enhancer of Zeste protein. *Genes Dev.* **16**, 2893-2905.
Laible, G., Wolf, A., Dorn, R., Reuter, G., Nislow, C., Lebersorger, A., Popkin, D., Pillus, L. and Jenuwein, T. (1997). Mammalian homologues of the Polycomb-group gene Enhancer of zeste mediate gene silencing in Drosophila heterochromatin and at S. cerevisiae telomeres. *EMBO J.* **16**, 3219-3232.
Lee, J., Inoue, K., Ono, R., Ogonuki, N., Kohda, T., Kaneko-Ishino, T., Ogura, A. and Ishino, F. (2002). Erasing genomic imprinting memory in mouse clone embryos produced from day 11.5 primordial germ cells. *Development* **129**, 1807-1817.
Maison, C., Bailly, D., Peters, A. H., Quivy, J. P., Roche, D., Taddei, A., Lachner, M., Jenuwein, T. and Almouzni, G. (2002). Higher-order structure in pericentric heterochromatin involves a distinct pattern of histone modification and an RNA component. *Nat. Genet.* **30**, 329-334.
Mak, W., Baxter, J., Silva, J., Newall, A. E., Otte, A. P. and Brockdorff, N. (2002). Mitotically stable association of polycomb group proteins eed and enx1 with the inactive X chromosome in trophoblast stem cells. *Curr. Biol.* **12**, 1016-1020.
Mayer, W., Niveleau, A., Walter, J., Fundele, R. and Haaf, T. (2000). Demethylation of the zygotic paternal genome. *Nature* **403**, 501-502.
Monk, M., Boubelik, M. and Lehnert, S. (1987). Temporal and regional changes in DNA methylation in the embryonic, extraembryonic and germ cell lineages during mouse embryo development. *Development* **99**, 371-382.
Morin-Kensicki, E. M., Faust, C., LaMantia, C. and Magnuson, T. (2001). Cell and tissue requirements for *eed* during mouse gastrulation and organogenesis. *Genesis* **31**, 142-146.
Muller, J., Hart, C. M., Francis, N. J., Vargas, M. L., Sengupta, A., Wild, B., Miller, E. L., O'Connor, M. B., Kingston, R. E. and Simon, J. A. (2002). Histone methyltransferase activity of a Drosophila polycomb group repressor complex. *Cell* **111**, 197-208.
Nichols, J., Zevnik, B., Anastassiadis, K., Niwa, H., Klewe-Nebenius, D., Chambers, I., Scholer, H. and Smith, A. (1998). Formation of pluripotent stem cells in the mammalian embryo depends on the POU transcription factor Oct4. *Cell* **95**, 379-391.
Nishioka, K., Chuikov, S., Sarma, K., Erdjument-Bromage, H., Allis, C. D., Tempst, P. and Reinberg, D. (2002). Set9, a novel histone H3 methyltransferase that facilitates transcription by precluding histone tail modifications required for heterochromatin formation. *Genes Dev.* **16**, 479-489.
Nonchev, S. and Tsanev, R. (1990). Protamine-histone replacement and DNA replication in the male mouse pronucleus. *Mol. Reprod. Dev.* **25**, 72-76.
O'Carroll, D., Erhardt, S., Pagani, M., Barton, S. C., Surani, M. A. and Jenuwein, T. (2001). The polycomb-group gene Ezh2 is required for early mouse development. *Mol. Cell. Biol.* **21**, 4330-4336.
Oswald, J., Engemann, S., Lane, N., Mayer, W., Olek, A., Fundele, R., Dean, W., Reik, W. and Walter, J. (2000). Active demethylation of the paternal genome in the mouse zygote. *Curr. Biol.* **10**, 475-478.
Paro, R. and Harte, P. J. (1996). The role of Polycomb group and trithorax group chromatin complexes in the maintenance of determined cell states. In *Epigenetic mechanisms of gene regulation* (ed. V. E. A. Russo, R. A. Martienssen, and A. D. Riggs), pp. 507-528. Plainview, New York: Cold Spring Harbor Laboratory Press.
Peters, A. H., O'Carroll, D., Scherthan, H., Mechtler, K., Sauer, S., Schofer, C., Weipoltshammer, K., Pagani, M., Lachner, M., Kohlmaier, A., Opravil, S., Doyle, M., Sibilia, M. and Jenuwein, T. (2001). Loss of the Suv39h histone methyltransferases impairs mammalian heterochromatin and genome stability. *Cell* **107**, 323-337.
Plath, K., Fang, J., Mlynarczyk-Evans, S. K., Cao, R., Worringer, K. A., Wang, H., de la Cruz, C. C., Otte, A. P., Panning, B. and Zhang, Y. (2003). Role of histone H3 lysine 27 methylation in X inactivation. *Science* **300**, 131-135.
Rea, S., Eisenhaber, F., O'Carroll, D., Strahl, B. D., Sun, Z. W., Schmid, M., Opravil, S., Mechtler, K., Ponting, C. P., Allis, C. D. and Jenuwein, T. (2000). Regulation of chromatin structure by site-specific histone H3 methyltransferases. *Nature* **406,** 593-599.
Reik, W. and Walter, J. (2001). Genomic imprinting: parental influence on the genome. *Nat. Rev. Genet.* **2**, 21-32.
Rossant, J. (2001). Stem cells from the mammalian blastocyst. *Stem Cells* **194**, 77-82.
Santos, F., Hendrich, B., Reik, W. and Dean, W. (2002). Dynamic reprogramming of DNA methylation in the early mouse embryo. *Dev. Biol.* **241**, 172-182.
Schumacher, A., Faust, C. and Magnuson, T. (1996). Positional cloning of a global regulator of anterior-posterior patterning in mice. *Nature* **383**, 250-253.
Sewalt, R. G., van der Vlag, J., Gunster, M. J., Hamer, K. M., den Blaauwen, J. L., Satijn, D. P., Hendrix, T., van Driel, R. and Otte, A. P. (1998). Characterization of interactions between the mammalian polycomb-group proteins Enx1/EZH2 and EED suggests the existence of different mammalian polycomb-group protein complexes. *Mol. Cell. Biol.* **18**, 3586-3595.
Seydoux, G. and Strome, S. (1999). Launching the germline in Caenorhabditis elegans: regulation of gene expression in early germ cells. *Development* **126**, 3275-3283.
Silva, J., Mak, W., Zvetkova, I., Appanah, R., Nesterova, T. B., Webster, Z., Peters, A. H., Jenuwein, T., Otte, A. P. and Brockdorff, N. (2003). Establishment of histone H3 methylation on the inactive x chromosome

requires transient recruitment of eed-enx1 polycomb group complexes. *Dev. Cell* **4**, 481-495.

Strahl, B. D. and Allis, C. D. (2000). The language of covalent histone modifications. *Nature* **403**, 41-45.

Su, I., Basavaraj, A., Krutchinsky, A. N., Hobert, O., Ullrich, A., Chait, B. T. and Tarakhovsky, A. (2003). Ezh2 regulates B cell development through histone H3 methylation and IgH gene rearrangement. *Nat. Immunol.* **4**, 124-131.

Surani, M. A. (2001). Reprogramming of genome function through epigenetic inheritance. *Nature* **414**, 122-128.

Tachibana, M., Sugimoto, K., Nozaki, M., Ueda, J., Ohta, T., Ohki, M., Fukuda, M., Takeda, N., Niida, H., Kato, H. and Shinkai, Y. (2002). G9a histone methyltransferase plays a dominant role in euchromatic histone H3 lysine 9 methylation and is essential for early embryogenesis. *Genes Dev.* **16**, 1779-1791.

Tamaru, H. and Selker, E. U. (2001). A histone H3 methyltransferase controls DNA methylation in Neurospora crassa. *Nature* **414**, 277-283.

Tie, F., Furuyama, T., Prasad-Sinha, J., Jane, E. and Harte, P. J. (2001). The Drosophila Polycomb Group proteins ESC and E(Z) are present in a complex containing the histone-binding protein p55 and the histone deacetylase RPD3. *Development* **128**, 275-286.

van der Vlag, J. and Otte, A. P. (1999). Transcriptional repression mediated by the human polycomb-group protein EED involves histone deacetylation. *Nat Genet* **23**, 474-478.

Varambally, S., Dhanasekaran, S. M., Zhou, M., Barrette, T. R., Kumar-Sinha, C., Sanda, M. G., Ghosh, D., Pienta, K. J., Sewalt, R. G., Otte, A. P., Rubin, M. A. and Chinnaiyan, A. M. (2002). The polycomb group protein EZH2 is involved in progression of prostate cancer. *Nature* **419**, 624-629.

Vidal, F., Sage, J., Cuzin, F. and Rassoulzadegan, M. (1998). Cre expression in primary spermatocytes: a tool for genetic engineering of the germ line. *Mol. Reprod. Dev.* **51**, 274-280.

Vrana, P. B., Guan, X. J., Ingram, R. S. and Tilghman, S. M. (1998). Genomic imprinting is disrupted in interspecific Peromyscus hybrids. *Nat. Genet.* **20**, 362-365.

Wang, H., Cao, R., Xia, L., Erdjument-Bromage, H., Borchers, C., Tempst, P. and Zhang, Y. (2001a). Purification and functional characterization of a histone H3-lysine 4-specific methyltransferase. *Mol. Cell* **8**, 1207-1217.

Wang, J., Mager, J., Chen, Y., Schneider, E., Cross, J. C., Nagy, A. and Magnuson, T. (2001b). Imprinted X inactivation maintained by a mouse Polycomb group gene. *Nat. Genet.* **28**, 371-375.

Werren, J. H. and Hatcher, M. J. (2000). Maternal-zygotic gene conflict over sex determination: effects of inbreeding. *Genetics* **155**, 1469-1479.

Wutz, A. and Jaenisch, R. (2000). A shift from reversible to irreversible X inactivation is triggered during ES cell differentiation. *Mol. Cell* **5**, 695-705.

Yang, L., Xia, L., Wu, D. Y., Wang, H., Chansky, H. A., Schubach, W. H., Hickstein, D. D. and Zhang, Y. (2002). Molecular cloning of ESET, a novel histone H3-specific methyltransferase that interacts with ERG transcription factor. *Oncogene* **21**, 148-152.